COLOCATED MIMO RADAR: BEAMFORMING TRANSMISSION, WAVEFORM MODELING, TARGET PARAMETER ESTIMATION

RANDRIANANDRASANA Marie Emile [1], RANDRIAMITANTSOA Paul Auguste[2], RANDRIAMITANTSOA Andry Auguste[3]

[1]*Dept. of Telecommunication, Antsirabe Vankinankaratra High Education Institute, University of Antananarivo, Madagascar,*

[2]*Dept. of Telecommunication, High School Polytechnic of Antananarivo, University of Antananarivo, Madagascar,*

[3]*Dept. of Telecommunication, High School Polytechnic of Antananarivo, University of Antananarivo, Madagascar,*

ABSTRACT

This work focused on the topic related to emerging MIMO radar technology. A new method to jointly solve the problem of designing the beam pattern as well as the waveform is detailed. Uses of different mapping functions, Gaussian and random variables are mapped onto waveforms with different modulation schemes and the relationships between the cross-correlation of Gaussian VR and these waveforms are derived. We have introduced the estimation of the reflection coefficient, the Doppler shift and the localization of a moving target in the presence of interferers. By exploiting a 2D-FFT transformation, we avoided a complex two-dimensional resolution finding process.

Keywords: radar, MIMO, modulation, interferer, 2D-FFT

1. INTRODUCTION

Radar, an acronym for Radio Detection and Ranging, detects and locates targets in a limited volume in space by transmitting electromagnetic energy and processing reflected echoes [1]. Other target characteristics such as speed, shape and composition can also be extracted. Introduced towards the end of the 19th century, the concept of detecting the presence of metallic objects at a distance by means of radio waves aroused much interest, mainly in the military field, and was considerably improved during the two world wars. [2]. Nowadays, radars are used more and more in many fields such as speed-gun, short-term weather forecasts as well as geological observations [3].

2. MIMO RADAR

MIMO radar can transmit independent or partially correlated waveforms [4]. As in communications, MIMO technology has greatly improved the performance of the radar system. For example, the MIMO radar can identify multiple targets n_T times [5]. In addition, MIMO radars benefit from virtual arrays [6] and offer additional degrees of freedom [7], which can be exploited for more, better parametric identifiable, higher spatial resolution and beam pattern design more complex transmissions.

Consider a collocated MIMO radar of nT transmit and receive antennas. If $x_m(n)$ is the baseband signal emitted by antenna m at a frequency $f_c = \frac{c}{\lambda_c}$, the signal received by a target located at an angle θ_t in a far field is:

$$r(n, \theta_t) = a_T^T(\theta_t)x(n), \;\; n = 1,2, \dots \dots, N, \tag{1}$$

where N denotes the total number of symbols transmitted from each antenna, $x(n)$ is the vector of symbols transmitted at time index n:

$$x(n) = [x_1(n) \quad x_2(n) \quad \dots \quad x_{nT}(n)]^T, \tag{2}$$

and $a_T(\theta)$ is the transmission direction vector which takes into account the delay relative to each antenna and is expressed as follows:

$$a_T(\theta) = \left[e^{j\frac{2\pi}{\lambda_c}T_1(\theta)} \quad e^{j\frac{2\pi}{\lambda_c}T_2(\theta)} \quad \dots \quad e^{j\frac{2\pi}{\lambda_c}T_{nT}(\theta)}\right]^T. \tag{3}$$

Using equation (1), the power transmitted in a specific direction θ is defined as

$$P(\theta) = E\{a_T^T(\theta)x(n)x^H(n)a_T^*(\theta)\} = a_T^T(\theta)Ra_T^*(\theta), \quad (4)$$

where R is the covariance matrix of the transmitted waveforms. If the waveforms are orthogonal, i.e. $R = \ln(T)$, power is equally transmitted in all directions and adaptive techniques can be applied without the need for counting .

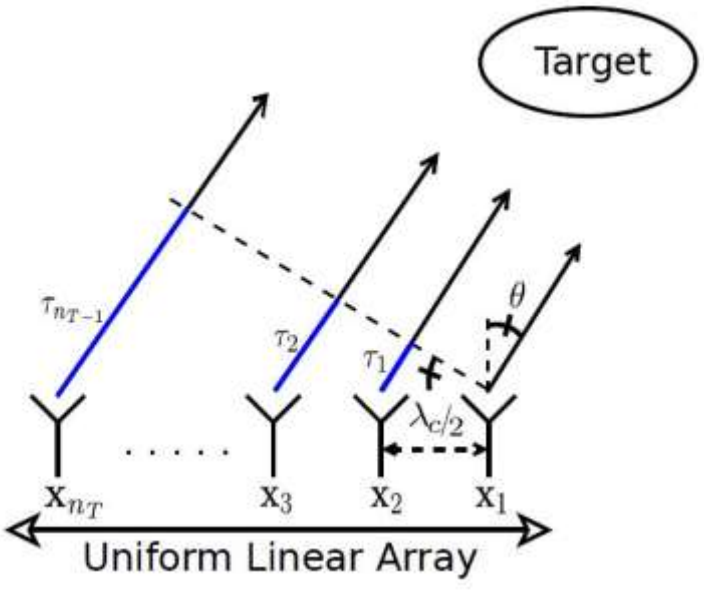

Fig 1. : Diagram of a uniform linear radar

If we consider a ULA (Uniform Linear Array) radar with a half-wavelength spacing between each element (see Figure 1), the expression for the excess distance $\tau_i(\theta)$ traveled by the signal emitted by the antenna i becomes:

$$\tau_i(\theta) = (i-1)\frac{\lambda_c}{2}\sin(\theta), \quad (5)$$

and the expression of the direction vector a_T becomes:

$$a_T(\theta) = [1 \quad e^{j\pi sin(\theta)} \quad \dots \quad e^{j(n_T-1)\pi sin(\theta)}] \quad (6)$$

Assuming that the target has a reflection coefficient β_t and moves with a radial velocity v_r, it produces a normalized Doppler shift f_{dt} such that:

$$f_{dt} = \frac{v_r}{c}f_c. \quad (7)$$

By defining the direction receiving vector a_R as:

$$a_R(\theta) = [1 \quad e^{i\pi sin(\theta)} \quad \dots \quad e^{i(n_R-1)\pi sin(\theta)}], \quad (8)$$

Echoes reflected from the target are designated by:

$$y_t(n) = \beta_t e^{j2\pi f_{dt}n}a_R(\theta_t)a_T^T(\theta_t)x(n). \quad (9)$$

Moreover, let L be the number of static interferers located at angles θ_1 to θ_L and with a reflection coefficient β_1 to β_L. In the presence of a white Gaussian noise centered v, the received signals can be expressed in vector form:

$$y(n) = \beta_t e^{j2\pi f_{dt}n}a_R(\theta_t)a_T^T(\theta_t)x(n) + \sum_{i=1}^{L}\beta_i a_R(\theta_i)a_T^T(\theta_i)x(n) + v(n), n = 1,2,\dots,N \quad (10)$$

3. BEAMFORMING TRANSMISSION AND WAVEFORM DESIGN

Beampattern matching involves designing waveforms with the specific properties of cross-correlation to approximate a desired beam. Usually the desired beam is used to maximize the transmitted power in the region of interest and minimize it in all other directions. As shown in equation (1), the baseband signal received at a location θ_k is defined as:

$$\mathrm{r(n,\theta_k) = a_T^T(\theta_k)x(n); n = 1,2,\dots\dots\dots\dots N} \quad (11)$$

Thus, the received power at location θ_k is expressed as:

$$P(\theta_k) = \mathrm{E\{a_T^T(\theta_k)x(n)x^H}(n)a_T^*(\theta_k)\} = \mathrm{a_T^T(\theta_k)\mathbf{R}a_T^*(\theta_k)}, \quad (12)$$

where $\boldsymbol{R}$ is the correlation matrix of the transmitted waveforms. To reach the desired bundle $\phi(\theta)$, the covariance matrix $\boldsymbol{R}$ should minimize the following constrained problem:

$$\min_{\boldsymbol{R},\alpha}\frac{1}{K}\sum_{k=1}^{K}\left(a_T^T(\theta_k)\boldsymbol{R}a_T^*(\theta_k) - \alpha\phi(\theta_k)\right)^2 \quad (13)$$

subject to $v^H\boldsymbol{R}v > 0$, for all v

$$\boldsymbol{R}(n,n) = c, \text{ for } m = 1,2,\dots\dots\dots N, \quad (14)$$

where K is the number of subdivisions of the region of interest, α is a weighting factor and c is the power transmitted by each antenna. Since R should be a positive covariance matrix, the first constraint is straightforward. Also, the second constraint must be met to achieve maximum energy efficiency. Moreover, depending on the parity of the desired bundle $\phi(\theta)$ the designed covariance matrix R can contain reals or complex elements.
Once R has been synthesized, the matrix of waveforms $\mathrm{X} = [\mathrm{x}_1 \quad \mathrm{x}_2 \quad \cdots \quad \mathrm{x}_\mathrm{N}]$ can easily be obtained using the Gaussian RV as follows:

$$\mathrm{X} = \chi \Lambda^{\frac{1}{2}} W^H \tag{15}$$

where $\mathrm{X} \in \mathrm{C}^{\mathrm{L}\times\mathrm{N}}$, x_n is a vector of symbols transmitted by antenna n, χ is a matrix with zero mean and unit variance Gaussian VR, $\Lambda \in \mathcal{R}^{N\times N}$ is the diagonal eigenvalue matrix and W is the eigenvector matrix of R. As X is Gaussian, it cannot guarantee a finite alphabet solution and may have a high PAPR.

4. GENERATION OF FINISHED ALPHABET SIGNALS FROM REAL GAUSSIANS VR

Let ψ_{pq} be the cross-correlation between the finite alphabet waveforms $y_p(n)$ and $y_q(n)$ and ρ_{pq} the cross-correlation between the null mean Gaussian sharp shapes $x_p\,(n)$ and $x_q\,(n)$. Thanks to a nonlinear function $f\,(.)$ Without memory, the Gaussian RV xp and xq can be mapped on the FACE or FANCE RV $y_p = f(x_p)$ and $y_q = f(x_q)$. The relationship between the cross-correlation coefficients ψ_{pq} and ρ_{pq} is given by:

$$\psi_{pq} \equiv \int_{-\infty}^{+\infty}\int_{-\infty}^{+\infty} y_p y_q^* p(x_p, x_q, \rho_{pq}) dx_p dx_q, \tag{16}$$

where $p(x_p, x_q, \rho_{pq}) \equiv \frac{1}{2\pi\sigma_p\sigma_q\sqrt{1-\rho_{pq}^2}} e^{-\frac{1}{2\left(1-\rho_{pq}^2\right)}\left[\left(\frac{x_p}{\sigma_p}\right)^2 - 2\left(\frac{x_p}{\sigma_p}\right)\left(\frac{x_q}{\sigma_q}\right) + \left(\frac{x_q}{\sigma_p}\right)^2\right]}$ is the common PDF of x_p and x_q. Here, σ_p^2 and σ_q^2 denote the variance of the Gaussian random variables x_p and x_q, respectively. To separate the double integration in equation (16), the Hermite polynomials are used as in [8] to obtain the following expression:

$$\psi_{pq} = \sum_{n=0}^{+\infty} \frac{\rho_{pq}^n}{2^n n!} \int_{-\infty}^{+\infty} f(x_p) H_n\left(\frac{x_p}{\sigma_p\sqrt{2}}\right) p(x_p) dx_p \int_{-\infty}^{+\infty} f(x_q) H_n\left(\frac{x_q}{\sigma_q\sqrt{2}}\right) p(x_q) dx_q \tag{17}$$

where $p\,(x)$ is the PDF of the Gaussian RV real and $H_n\,(x)$ are the Hermite polynomial physicists. In our case, like x_p and x_q. have the same variance, i.e. $\sigma_p^2 = \sigma_q^2 = 1$, the above expression can be further simplified to:

$$\psi_{pq} = \frac{1}{2\pi}\sum_{n=0}^{+\infty}\left|\int_{-\infty}^{+\infty} f(x) H_n\left(\frac{x}{\sqrt{2}}\right) e^{\frac{x^2}{2}} dx\right|^2 \frac{\rho_{pq}^n}{2^n n!} \tag{18}$$

If M is the number of alphabets in a modulation scheme, the PDF region is divided into M regions using the delimiters $\alpha_m, m = -\frac{M}{2}, \ldots, 0, \ldots, \frac{M}{2}$. Depending on the application, the modulation scheme may contain symbols with a different appearance probability: $p_m, m = -\frac{M}{2}, \ldots, -1, 1, \ldots, \frac{M}{2}$ .Therefore, the α_m delimiters are chosen such as:

$$\begin{cases} \alpha \pm \dfrac{M}{2} = \pm\infty, \\ \displaystyle\int_{\sqrt{2}\alpha_{m-1}}^{\sqrt{2}\alpha_m} \frac{1}{\sqrt{2\pi}} e^{-\frac{x^2}{2}} = p_m \end{cases} \tag{19}$$

In this work, we will focus on the generation of equiprobable symbols, i.e. $p_m = \frac{1}{M}$. Thus, taking into account the symmetry of the Gaussian PDF function, we can deduce that:

$$\begin{cases} \alpha_0 = 0 \\ \alpha_i = -\alpha_{-i} \end{cases} \text{for } = 1,2, \ldots, \frac{M}{2} \tag{20}$$

Figure 2 illustrates how the Gaussian PDF is divided into 8 regions of equal area to generate 8 equiprobable symbols. Moreover, to ensure that ψ_{pq} spans the closed set [-1,1], the memoryless nonlinear mapping function $f(x)$ must be an odd function. Knowing that $H_n(-x) = (-1)^n H_n(x)$ [9], we substitute $\tilde{x} = \frac{x}{\sqrt{2}}$ and the relationship between the correlation of Gaussian and mapped RV (18) can be reformulated as:

$$\begin{aligned} \psi_{pq} &= \frac{1}{\pi}\sum_{n=0}^{+\infty}\frac{\rho_{pq}^n}{2^n n!}\left|\int_0^{+\infty} f(\tilde{x})\left(H_n(\tilde{x}) - (-1)H_n(\tilde{x})\right)e^{-\tilde{x}^2} d\tilde{x}\right|^2 \\ &= \frac{2}{\pi}\sum_{n=0}^{+\infty}\frac{\rho_{pq}^{2n+1}}{2^{2n}(2n+1)!}\left|\int_0^{+\infty} f(\tilde{x}) H_{2n+1}(\tilde{x}) e^{-\tilde{x}^2} d\tilde{x}\right|^2 \end{aligned} \tag{21}$$

By mapping Gaussian RV between the region $]\,\alpha_{m-1}, \alpha_m\,[$ onto a constellation symbol s_m, the above expression can be split into a sum of integrals as follows:

$$\psi_{pq} = \frac{2}{\pi}\sum_{n=0}^{+\infty}\frac{\rho_{pq}^{2n+1}}{2^{2n}(2n+1)!}\left|\sum_{m=1}^{\frac{M}{2}} s_m \int_{\alpha_{m-1}}^{\alpha_m} H_{2n+1}(\tilde{x})e^{-\tilde{x}^2}d\tilde{x}\right|^2 \tag{22}$$

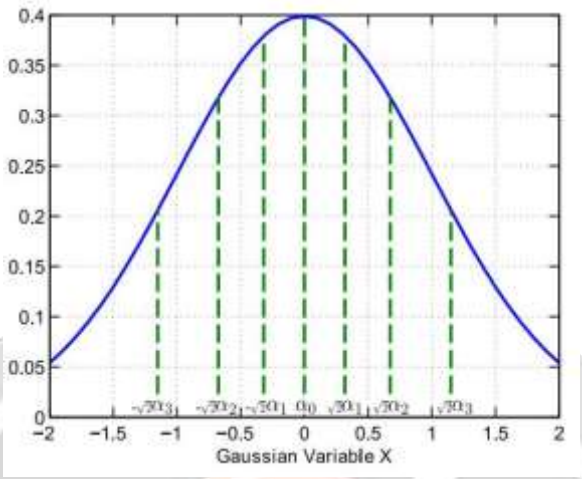

Fig 2: Gaussian PDF divided into 8 equiprobable regions

The integrals of equation (22) can be expressed as:

$$\begin{aligned}\int_{\alpha_{m-1}}^{\alpha_m} H_{2n+1}(\tilde{x})e^{-\tilde{x}^2}d\tilde{x} &= \int_0^{\alpha_m} H_{2n+1}(\tilde{x})e^{-\tilde{x}^2}d\tilde{x} \\ &- \int_0^{\alpha_{m-1}} H_{2n+1}(\tilde{x})e^{-\tilde{x}^2}dx = (-1)^n\frac{(2n)!}{n!}\widetilde{\left(a_n(\alpha_{m-1}) - a_n(\alpha_m)\right)}\end{aligned} \tag{23}$$

where $a_n(\alpha_m) = {}_1F_1\left(n+\frac{1}{2},\frac{1}{2},-\alpha_m^2\right)$ is Kummer's confluent hypergeometric function [10]. To illustrate the behavior of the power series $a_n(\alpha)$, Figure 3 shows the effect of the index n on its pseudo-period. The power series a_n reaches lower values when α, its oscillation frequency and its index increase. Using (23), the relation in (22) can finally be written as follows:

$$\psi_{pq} = \mathcal{F}(\rho_{pq}) = \frac{2}{\pi}\sum_{n=0}^{+\infty}\frac{\rho_{pq}^{2n+1}(|2n-1|)!!}{(2n+1)(2n)!!}\left|\sum_{m=1}^{\frac{M}{2}} s_m\left(a_n(\alpha_{m-1}) - a_n(\alpha_m)\right)\right|^2 \tag{24}$$

Since all the terms of the infinite sum of (24) are positive, with the use of the Schur product theorem [11], we can say that if the scalar ρ_{pq} is replaced by a positive semi-defined matrix $\boldsymbol{\mathcal{R}_g}$, the corresponding matrix on the left side is guaranteed to be positive and semi-defined.

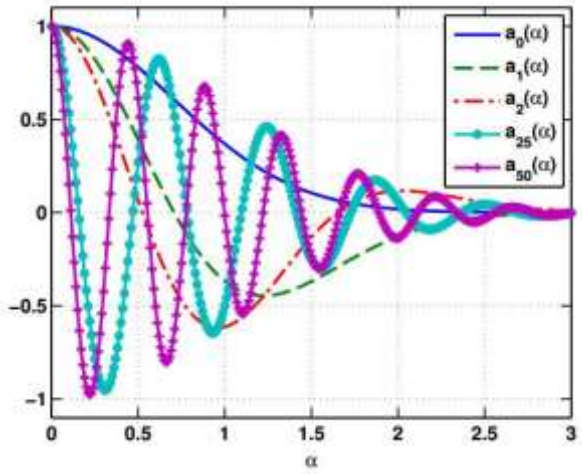

Fig 3: The behavior of the series $a_n(\alpha)$ as a function of α

It should also be noted that the relationship between the Gaussian cross-correlation and the corresponding RV depends on the chosen delimiters, $\alpha_m, m = 1, \dots, \frac{M}{2} - 1$, and the symbols $s_m, m = 1, \dots, \frac{M}{2}$ assigned to each region.

In the next section, real Gaussian RV is mapped onto the memoryless complex exponential functions to generate PSK-modulated RV and match the symmetric beam patterns. These results will be used later to generate PAM and QAM modulated waveforms.

5. GENERATION OF PSK SIGNALS FROM REAL GAUSSIAN RANDOM VARIABLES

5.1 BPSK wave

To generate BPSK waveforms, Gaussian random variables are mapped into symbols using the mapping function above:

$$y = f(x) = sign(x) \tag{25}$$

where $sign\ (\cdot)$ is the sign function.

In this case, using $\int_0^{+\infty} H_{2n+1}(\tilde{x}) e^{-\tilde{x}^2} d\tilde{x} = (-1)^n \frac{(2n)!}{n!}$, we can deduce the relationship between the correlation of Gaussian VR and BPSK demonstrated in [12]

$$\psi_{pq} = \frac{2}{\pi} \sum_{n=0}^{+\infty} \frac{\rho_{pq}^{2n+1} (|2n-1|)!!}{(2n+1)(2n)!!} = \frac{2}{\pi} \sin^{-1}(\rho_{pq}) \tag{26}$$

5.2 QPSK wave

To generate QPSK waveforms, the PDF of Gaussian VR is divided into four equal regions and mapped to the symbols $s_m = \left\{e^{-j\frac{\pi}{4}}, e^{-j\frac{3\pi}{4}}, e^{j\frac{\pi}{4}}, e^{j\frac{3\pi}{4}}\right\}$ using the function

$$\begin{aligned} y = f(x) &= e^{\left[j\frac{\pi}{4}\left(2sign(x) - sign\left(1 - \frac{x^2}{2\alpha_1^2}\right)\right)\right]} \\ &= \begin{cases} e^{j\frac{\pi}{4}} & if\ x \in [0, \sqrt{2}\alpha_1] \\ e^{j\frac{3\pi}{4}} & if\ x > \sqrt{2}\alpha_1 \\ -f(-x) & if\ x < 0 \end{cases} \end{aligned} \tag{27}$$

To ensure that all symbols are equiprobable, the delimiter $\alpha_1 = 0{,}4769$ is determined using the Inverse Cumulative Distribution Function (ICDF) associated with the standard normal distribution, also known as the probit function. Using (22), the cross-correlation relationship between Gaussian RV and QPSK can be deduced as shown below:

$$\psi_{pq} = \frac{2}{\pi} \sum_{n=0}^{+\infty} \frac{\rho_{pq}^{2n+1}}{2^{2n}(2n+1)!} \left| e^{j\frac{\pi}{4}} \int_0^{\alpha_1} H_{2n+1}(\tilde{x}) e^{-\tilde{x}^2} d\tilde{x} + e^{j\frac{3\pi}{4}} \int_{\alpha_1}^{\infty} H_{2n+1}(\tilde{x}) e^{-\tilde{x}^2} d\tilde{x} \right|^2 \tag{28}$$

Using the result in (23), (28) we can rephrase it as:

$$\begin{aligned} \psi_{pq} &= \frac{2}{\pi} \sum_{n=0}^{+\infty} \frac{\rho_{pq}^{2n+1} (|2n-1|)!!}{(2n+1)(2n)!!} \left| e^{j\frac{\pi}{4}} (1 - a_n(\alpha_1)) + e^{j\frac{3\pi}{4}} a_n(\alpha_1) \right|^2 \\ &= \frac{2}{\pi} \sum_{n=0}^{+\infty} \frac{\rho_{pq}^{2n+1} (|2n-1|)!!}{(2n+1)(2n)!!} \left(1 - 2a_n(\alpha_1) + 2a_n(\alpha_1)\right) \end{aligned} \tag{29}$$

5.3 8-PSK wave

Similarly, applying the probit function, the Gaussian RV are divided into eight regions and mapped over $s_m = \left\{e^{-j\frac{\pi}{8}}, e^{-j\frac{3\pi}{8}}, e^{-j\frac{5\pi}{8}}, e^{-j\frac{7\pi}{8}}, e^{j\frac{\pi}{8}}, e^{j\frac{3\pi}{8}}, e^{j\frac{5\pi}{8}}, e^{j\frac{7\pi}{8}}\right\}$ using the following mapping function:

$$f(x) = e^{\left[j\frac{\pi}{8}\left(4\ sign\ (x) - 2\ sign\left(1 - \frac{x^2}{2\alpha_2^2}\right) - sign\left(\left(1 - \frac{x^2}{2\alpha_1^2}\right)\left(1 - \frac{x^2}{2\alpha_2^2}\right)\left(1 - \frac{x^2}{2\alpha_3^2}\right)\right)\right)\right]},$$

$$\begin{cases} e^{j\frac{\pi}{8}} & if\ x \in [0, \sqrt{2}\alpha_1], \\ e^{j\frac{3\pi}{8}} & if\ x \in]\sqrt{2}\alpha_1, \sqrt{2}\alpha_2], \\ e^{j\frac{5\pi}{8}} & if\ x \in]\sqrt{2}\alpha_2, \sqrt{2}\alpha_3], \\ e^{j\frac{7\pi}{8}} & if\ x > \sqrt{2}\alpha_3\ , \\ -f(-x) & if\ x < 0 \end{cases} \tag{30}$$

Where, for 8-PSK equiprobable symbols, the delimiters are:

$$\begin{cases}\alpha_1 = 0.2253 \\ \alpha_2 = 0.4769 \\ \alpha_3 = 0.8134\end{cases} \tag{31}$$

In this case, the relationship between the cross-correlation of Gaussian RV and 8-PSK can be derived using (24) as follows:

$$\psi_{pq} = \frac{2}{\pi}\sum_{n=0}^{+\infty}\frac{\rho_{pq}^{2n+1}}{2^{2n}(2n+1)!}\left|e^{j\frac{\pi}{8}}\left(1-a_n(\alpha_1)\right)+e^{j\frac{3\pi}{8}}\left(a_n(\alpha_1)-a_n(\alpha_2)\right)+e^{j\frac{5\pi}{8}}\left(a_n(\alpha_2)-a_n(\alpha_3)\right)+e^{j\frac{7\pi}{8}}a_n(\alpha_3)\right|^2 \tag{32}$$

Figure 4 shows the cross-correlation relationship between Gaussian and FACE alphabets (i.e. BPSK, QPSK and 8-PSK). It can be noticed that the absolute value of the cross-correlation of higher PSK signals is always lower than the absolute value of BPSK symbols.

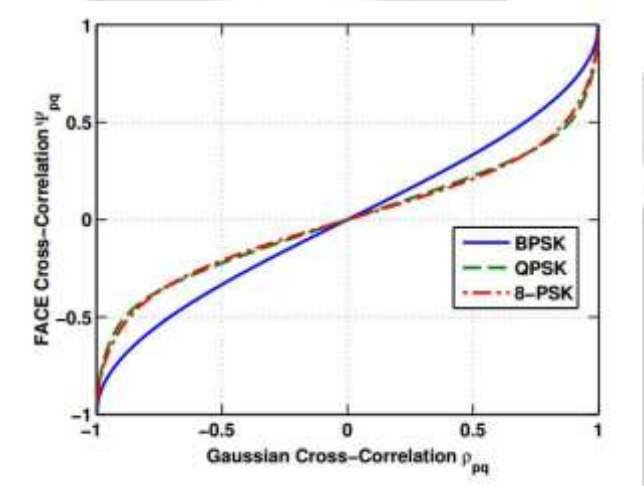

Fig 4: Graph of the relationship between Gaussian RV and FACE

6. GENERATION OF PAM WAVEFORMS FROM REAL GAUSSIAN RANDOM VARIABLES

6.1 4-PAM

To generate the 4-PAM constellation symbols, the mapping function $f(\cdot)$ becomes:

$$y = f(x) = \frac{1}{\sqrt{5}}\left(2\,sign\,(x) - sign\left(x - \frac{x^3}{2\alpha_1^2}\right)\right) \tag{33}$$

$$\begin{cases}\dfrac{1}{\sqrt{5}} & if\ x \in [0, \sqrt{2}\alpha_1] \\ \dfrac{3}{\sqrt{5}} & if\ x > \sqrt{2}\alpha_1 \\ -f(-x) & if\ x < 0\end{cases} \tag{34}$$

where, as defined in subsection 5.2, the delimiter $\alpha_1 = 0{,}4769$. In this case, the relationship between Gaussian RV and 4-PAM symbols can be written as:

$$\psi_{pq} = \frac{2}{5\pi}\sum_{n=0}^{+\infty}\frac{\rho_{pq}^{2n+1}}{2^{2n}(2n+1)!}\left|\int_0^{\alpha_1} H_{2n+1}(\tilde{x})e^{-\tilde{x}^2}d\tilde{x} + 3\int_{\alpha_1}^{\infty} H_{2n+1}(\tilde{x})e^{-\tilde{x}^2}d\tilde{x}\right|^2 \tag{35}$$

Using the result of (23), the above relation can finally be expressed as:

$$\psi_{pq} = \frac{2}{5\pi}\sum_{n=0}^{+\infty}\frac{\rho_{pq}^{2n+1}(|2n-1|)!!}{(2n+1)(2n)!!}\left(1+4a_n(\alpha_1)+4a_n^2(\alpha_1)\right) \tag{36}$$

An approximation of the relationship can be found by minimizing the least squares problem. The following approximations have been found to give good results.

$$\psi_{pq} \approx \frac{2}{\pi}\frac{\sin^{-1}(\rho_{pq})}{0.71 + 0.45\rho_{pq}^2 + 1.05\rho_{pq}^4 + 0.89\rho_{pq}^6}$$
$$avec\ \rho_{pq} = \frac{\sin\left(\frac{\pi}{2}\psi_{pq}\right)}{0.33 - 0.25\psi_{pq}^2 - 0.38\psi_{pq}^4 - 0.30\psi_{pq}^6} \quad (37)$$

6.2 8-PAM

:Using the same delimiters as in (31), the standard normal PDF is split into 8 equiprobable regions and mapped to 8-PAM symbols as follows:

$$y = f(x) = \frac{1}{\sqrt{21}}\left(4\ sign\ (x) - 2\ sign\left(1 - \frac{x^2}{2\alpha_2^2}\right)\mu - sign\left(x\left(1 - \frac{x^2}{2\alpha_1^2}\right)\left(1 - \frac{x^2}{2\alpha_2^2}\right)\left(1 - \frac{x^2}{2\alpha_3^2}\right)\right)\right) \quad (38)$$

$$\begin{cases} \frac{1}{\sqrt{21}} & if\ x \in [0, \sqrt{2}\alpha_1] \\ \frac{3}{\sqrt{21}} & if\ x \in]\sqrt{2}\alpha_1, \sqrt{2}\alpha_2] \\ \frac{5}{\sqrt{21}} & if\ x \in]\sqrt{2}\alpha_1, \sqrt{2}\alpha_3] \\ \frac{7}{\sqrt{21}} & if\ x > \sqrt{2}\alpha_3 \\ -f(-x) & if\ x < 0 \end{cases}$$

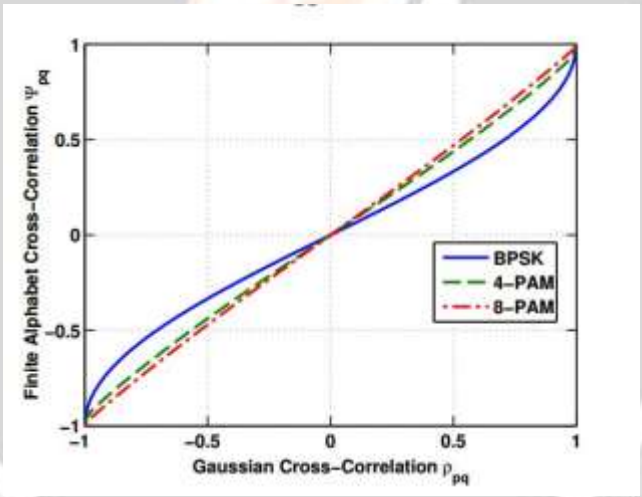

Fig 5: Graph of relationship between Gaussian search vehicles and FANCE

Applying (24) again in the case of 8-PAM symbols leads to the following relation:

$$\psi_{pq} = \frac{2}{21\pi}\sum_{n=0}^{+\infty}\frac{\rho_{pq}^{2n+1}}{2^{2n}(2n+1)!}\left|\left(1 - a_n(\alpha_1)\right) + 3\left(a_n(\alpha_1) - a_n(\alpha_2)\right) + 5\left(a_n(\alpha_2) - a_n(\alpha_3)\right) + 7a_n(\alpha_3)\right|^2 \quad (39)$$

$$\psi_{pq} = \frac{2}{21\pi}\sum_{n=0}^{+\infty}\frac{\rho_{pq}^{2n+1}}{2^{2n}(2n+1)!}\left|1 + 2\sum_{m=1}^{m=3}a_n(\alpha_m)\right|^2$$

Again, using a least squares method, the above relationship (39) can be approximated by:

$$\psi_{pq} \approx \frac{\rho_{pq}}{1.09 - 0.15\rho_{pq}^2 + 0.23\rho_{pq}^4 - 0.17\rho_{pq}^6} \quad (40)$$

$$\rho_{pq} = \frac{\sin\left(\frac{\pi}{2}\psi_{pq}\right)}{1.45 - 0.43\psi_{pq}^2 - 0.16\psi_{pq}^4 + 0.14\psi_{pq}^6} \quad (41)$$

A graph of derived relationships is shown in figure 5. It indicates that as the number of symbols increases, the relationship between the cross-correlation of Gaussian RV and PAM approaches the identity function. Thus, more covariance matrices will remain positive semi-definite when applying the inverse relation $\mathcal{F}^{-1}$.

7. GENERATION OF QAM SIGNALS FROM COMPLEX GAUSSIAN RANDOM VARIABLES

If the beam is non-symmetric, for optimal beam matching, R will be complex symmetric. For R to be complex, the waveforms must also be complex. Therefore, based on the PAM signal generation method, Gaussian complex random variables are mapped onto QAM alphabets. To generate an M-QAM RV from a complex Gaussian RV $x = x_R + jx_I$, the following mapping function is used:

$$y = f_Q(x)\frac{1}{\sqrt{2}}[f_P(x_R) + jf_P(x_I)] \tag{42}$$

where $f_Q(\cdot)$ denotes the mapping function used to generate M-QAM symbols while $f_P(.)$ denotes the mapping function used to generate $\sqrt{M} - PAM$ symbols.

Consider the semi-definite positive covariance matrix of the Gaussian complex RV $\boldsymbol{R}_g$. Since the covariance matrix is complex, using (15) the matrix of the corresponding correlated complex Gaussian RV can be written as follows

$$X = [\mathrm{x}_{\mathrm{R}_1} + j\mathrm{x}_{\mathrm{I}_1} \quad \mathrm{x}_{\mathrm{R}_2} + j\mathrm{x}_{\mathrm{I}_2} \quad \cdots \quad \mathrm{x}_{\mathrm{R}_N} + j\mathrm{x}_{\mathrm{I}_N}] \tag{43}$$

Let $\psi_{pq} = \psi_{R_{pq}} + j\psi_{I_{pq}}$ be the complex cross-correlation between the M-QAM RV $y_p(n)$ and $y_q(n)$, and $\rho_{pq} = \rho_{R_{pq}} + j\rho_{I_{pq}}$ let the complex cross-correlation between the Gaussian complex RV $x_p(n)$ and $x_q(n)$. Using (42), we can write:

$$\begin{aligned}\psi_{R_{pq}} &= \frac{1}{2}E\left\{f_P\left(x_{R_p}\right)f_P\left(x_{R_q}\right) + f_P\left(x_{I_p}\right)f_P\left(x_{I_q}\right)\right\}\\ \psi_{R_{pq}} &= \frac{1}{2}E\left\{f_P\left(x_{I_p}\right)f_P\left(x_{R_q}\right) - f_P\left(x_{R_p}\right)f_P\left(x_{I_q}\right)\right\}\end{aligned} \tag{44}$$

Using a whitening transformation, the waveform vector X can satisfy the following relationship:

$$E\left\{x_{R_p}x_{R_q}\right\} = E\left\{x_{I_p}x_{I_q}\right\} \tag{45}$$

$$E\left\{x_{R_p}x_{I_q}\right\} = -E\left\{x_{I_p}x_{R_q}\right\} \tag{46}$$

Thus, we can write:

$$\begin{aligned}\psi_{R_{pq}} &= E\left\{f_P\left(x_{R_p}\right)f_P\left(x_{R_q}\right)\right\}\\ \psi_{I_{pq}} &= E\left\{f_P\left(x_{I_p}\right)f_P\left(x_{R_q}\right)\right\}\end{aligned} \tag{47}$$

Using (23) and (24), the relationship between the real and imaginary parts of Gaussian complex RV and M-QAM symbols can be expressed as a Taylor series.

7.1 16-QAM

To generate 16-QAM signals from complex Gaussian RV, the following mapping function is used:

$$y = \frac{1}{\sqrt{2}}\left(f_{4PAM}(x_R) + jf_{4PAM}(x_R)\right) \tag{48}$$

where $f_{4PAM}(\cdot)$ is as defined in (34) and α is chosen equal to $\alpha_1 = 0{,}4769$ to guarantee the equivalence of the 16 symbols. Therefore, from (48) and Section 2.4, the relationship between the cross-correlation of Gaussian RV and 16-QAM symbols can be deduced as follows:

$$\begin{aligned}\psi_{R_{pq}} &= \frac{2}{5\pi}\sum_{n=0}^{+\infty}\frac{\rho_{R_{pq}}^{2n+1}(|2n-1|)!!}{(2n+1)(2n)!!}|1 + 2a_n(\alpha_1)|^2\\ \psi_{I_{pq}} &= \frac{2}{5\pi}\sum_{n=0}^{+\infty}\frac{\rho_{I_{pq}}^{2n+1}(|2n-1|)!!}{(2n+1)(2n)!!}|1 + 2a_n(\alpha_1)|^2\end{aligned} \tag{49}$$

7.2 64-QAM

The following mapping function is used to map complex Gaussian RV to 64-QAM symbols:

$$y = \frac{1}{\sqrt{2}}\left(f_{8PAM}(x_R) + jf_{8PAM}(x_R)\right) \tag{50}$$

where $f_{8PAM}(.)$ is as defined in (39) and delimiters are chosen as in (31). In this case, the relation between the cross-correlation of finite alphabets and the Gaussian RV becomes:

$$\psi_{R_{pq}} = \frac{2}{21\pi}\sum_{n=0}^{+\infty}\frac{\rho_{R_{pq}}^{2n+1}}{2^{2n}(2n+1)!}\left|1+2\sum_{m=1}^{m=3}a_n(\alpha_m)\right|^2$$
$$\psi_{I_{pq}} = \frac{2}{21\pi}\sum_{n=0}^{+\infty}\frac{\rho_{I_{pq}}^{2n+1}}{2^{2n}(2n+1)!}\left|1+2\sum_{m=1}^{m=3}a_n(\alpha_m)\right|^2 \quad (51)$$

8. PARAMETER ESTIMATION

As indicated in section 2, the signal received by a moving target located at a location at the angle θ_t in the presence of interferers is:

$$y(n) = \beta_t e^{j2\pi f_{dt}n}a_{\mathcal{R}}(\theta_t)a_T^T(\theta_t)\mathrm{x}(n) + \sum_{i=1}^{L}\beta a_{\mathcal{R}}(\theta_i)a_T^T\mathrm{x}(n) + \mathrm{v}(n), n = 1,2 \dots N \quad (52)$$

where $\mathrm{v}(n) = [\mathrm{v}_1(n) \quad \mathrm{v}_2(n) \quad \dots \quad \mathrm{v}_{\mathrm{n}_{\mathcal{R}}}(n)]^T$ is the white Gaussian complex vector zero-mean noise sample and σ_n^2 the variance. In MIMO radar, the waveforms transmitted by all antennas are independent. To maximize Signal to Interference Plus Noise (SINR), the received signal is multiplied with the beamformer weight vector, w, after which the received signal can be written:

$$w^H y(n) = \beta_i e^{j2\pi f_{dt}n}w^H a_{\mathcal{R}}(\theta_t)a_T^T(\theta_t)\mathrm{x}(n) + \sum_{i=1}^{L}\beta_i w^H a_{\mathcal{R}}(\theta_i)a_T^T(\theta_i)\mathrm{x(n)} + w^H\mathrm{v}(n) \quad (53)$$

If the covariance matrix of the interference plus noise term is denoted by R_{in}, the SINR can be defined as:

$$SNIR = \frac{|\beta_i|^2 E\left\{\left|e^{2j\pi f_{dt}n}\,w^H a_{\mathcal{R}}(\theta_t)a_T^T(\theta_t)\mathrm{x}(n)\right|^2\right\}}{w^H\mathcal{R}_{\mathrm{in}}\mathrm{w}} \quad (54)$$

where

$$\mathcal{R}_{in} = n_T\sum_{i=1}^{L}|\beta_i|^2 a_{\mathcal{R}}(\theta_i)a_{\mathcal{R}}^H(\theta_i) + \sigma_n^2 I_{n\mathcal{R}}\,. \quad (55)$$

8.1 Covariance matrix of unknown interference plus noise

If $\mathcal{R}_{in}$ is not known, one can find the Capon beamformer [13] to maximize the SINR ratio only from the received samples by solving the constraint of the following optimization problem [14]:

$$w = arg\min_{u}\ u^H\mathcal{R}_y u \quad \text{where } u^H a_R(\theta) = 1 \quad (56)$$

where $\mathcal{R}_y$ is the covariance matrix of the received prototypes. Solving it refers to the following beamformer expression:

$$w = \frac{R_y^{-1}a_R(\theta)}{a_R^H(\theta)R_y^{-1}a_R(\theta)} \quad (57)$$

To estimate the value of f_{dt}, θ_t and β_t the cost function to be minimized is as follows:

$$\{f_{dt}, \theta_t, \beta_t\} = arg\min_{f_d,\theta,\beta} E\left\{\left|w^H(\theta)y(n) - \beta e^{j2\pi f_d n}a_T^T(\theta)\mathrm{x(n)}\right|^2\right\} \quad (58)$$

The minimization of the previous cost function with respect to β can be found as:

$$\frac{\partial J_1}{\partial \beta^*} = E\{a_T^T\mathrm{x}(n)\mathrm{x}^H(n)a_T^*(\theta) - e^{-j2\pi f_d n}w^H y(n)\mathrm{x}^H(n)a_T^*(\theta)\} = 0 \quad (59)$$

Since all transmitted waveforms are independent, i.e., $E\{\mathrm{x}(n)\mathrm{x}^H(n)\} = I_{n_T}$ (59) refers to:

$$\beta(f_d,\theta) = \frac{1}{n_T}E\{e^{-j2\pi f_d n}w^H y(n)\mathrm{x}^H(n)a_T^*(\theta)\} \quad (60)$$

Using (57), (58) and (59), the cost function to be minimized to estimate f_{dt} and θ_t becomes:

$$J_2 = w^H(\theta)\boldsymbol{R_y}w(\theta) - \frac{1}{n_T}\left|E\{e^{-j2\pi f_d n}w^H y(n)\mathrm{x}^H(n)a_T^*(\theta)\}\right|^2$$
$$= \frac{1}{a_R^H(\theta)R_y^{-1}a_R(\theta)} - \frac{1}{n_T}\frac{\left|E\left\{e^{-j2\pi f_d n}R_y^{-1}y(n)\mathrm{x}^H(n)a_T^*(\theta)\right\}\right|^2}{\left(a_R^H(\theta)R_y^{-1}a_R(\theta)\right)^2} \quad (61)$$

As shown in appendix B, if there is no interferer, the respective minimization of f_d and θ is equivalent to the maximization of its second member only. Therefore, if $L = 0$ the problem can be simplified by maximizing the following cost function:

$$J_3 = \frac{\left|E\left\{e^{-j2\pi f_d n} a_R^H R_y^{-1} y(n) \mathrm{x}^H(n) a_T^*(\theta)\right\}\right|^2}{\left(a_R^H(\theta) R_y^{-1} a_R(\theta)\right)^2} \tag{62}$$

Assuming that $r^y(n) = R_y^{-1} y(n)$, the determination of the waiting operator can be written:

$$\begin{aligned} a(n) &= e^{-j2\pi f_d n} r^y(n) \mathrm{x}^H(n) a_T^*(\theta) \\ &= e^{-j2\pi f_d n} \sum_{q=1}^{n_R} r_q^y(n) e^{-j sin(\theta)(q-1)} \sum_{p=1}^{n_T} x_p^*(n) e^{-j sin(\theta)(p-1)} \\ &= e^{-j2\pi f_d n} \sum_{p=1}^{n_T} \sum_{q=1}^{n_R} r_q^y(n) x_p^*(n) e^{-j2\pi f_s (p+q-2)} \end{aligned} \tag{63}$$

Where $f_s = \frac{\sin(\theta)}{2}$. By combining the terms of identical frequency, we obtain:

$$\begin{aligned} (n) = \big(& x_1(n) r_1^y(n) + \left[x_1(n) r_2^y(n) + x_2(n) r_1^y(n)\right] e^{-j2\pi f_s} \\ &+ \left[x_1(n) r_3^y(n) + x_2(n) r_2^y(n) + x_3(n) r_1^y(n)\right] e^{-j2\pi f_s 2} + \cdots \\ &+ x_{n_T}(n) r_{n_R}^y(n) e^{-j2\pi f_s (n_T + n_R - 2)} \big) e^{-j2\pi f_d n} \end{aligned} \tag{64}$$

Therefore, one can find that:

$$E\{a(n)\} = \frac{1}{N} \sum_{n=0}^{N-1} \sum_{m=0}^{n_T + n_R - 2} f(n,m)\, e^{-j2\pi f_d n}\, e^{-j2\pi f_s} \tag{65}$$

Where $f(n,m) = \sum_{i=1}^{n_T} x_i(n) r_{m+2-i}^y(n)$

Interestingly, the right side of (65) is similar to the famous 2d-FFT expression. Therefore, if there is no interferer, the target and the Doppler frequency can be jointly estimated through the use of 2D-FFT as follows:

$$\hat{f}_{dt}, \hat{f}_{st} = arg \max_{f_d, f_s} \left| \frac{\sum_{n=0}^{N-1} \sum_{m=0}^{n_T + n_R - 2} f(n,m)\, e^{-j2\pi f_s} e^{-j2\pi f_d n}}{a_{f\ R}^{\ H}(f_s) R_y^{-1} a_{f\ \ R}(f_s)} \right| \tag{66}$$

Where :

$$a_{f_R}(f_s) = [1 \quad e^{2j\pi f s} \ldots\ldots \quad e^{2(n_R - 1) j \pi f_s}]^T \tag{67}$$

Finally, an estimator of θ_t can be formulated as follows:

$$\hat{\theta}_t = \sin^{-1}(2\ \hat{f}_{st}) \tag{68}$$

8.2 Known interference and noise covariance matrix

If the covariance matrix of the interference plus noise noise term R_{in} is known, the Capon beamformer that maximizes the SINR is the solution to the following optimization problem:

$$J = w^H R_{in} w + \lambda(w^H a_R(\theta) - 1) \tag{69}$$

where λ is the Lagrange multiplier. It can be derived as follows:

$$w = \frac{R_{in}^{-1} a_R(\theta)}{a_R^H R_{in}^{-1} a_R(\theta)} \tag{70}$$

As the above expression (70) is very similar to the one presented in (57), one can easily verify that the derivations of the estimators are also similar. Thus, in the presence of interferers, we substitute expression (70) for (61), and the cost function to be minimized becomes:

$$J_4 = \frac{a_R^H R_{in}^{-1} R_y R_n^{-1} a_R(\theta)}{\left(a_R^H(\theta) R_{in}^{-1} a_R(\theta)\right)^2} + \frac{1}{n_T} \frac{\left|E\left\{e^{-j2\pi f_d n} a_R^H R_y^{-1} y(n) \mathrm{x}^H(n) a_T^*(\theta)\right\}\right|^2}{\left(a_R^H(\theta) R_{in}^{-1} a_R(\theta)\right)^2} \tag{71}$$

Which, in the case of noise alone, can be simplified to maximize the cost function below:

$$J_5 = \frac{\left|E\left\{e^{-j2\pi f_d n} a_R^H R_y^{-1} y(n) \mathrm{x}^H(n) a_T^*(\theta)\right\}\right|^2}{\left(a_R^H(\theta) R_{in}^{-1} a_R(\theta)\right)^2} \tag{72}$$

Because the noise samples are uncorrelated, i.e. $R_{in} = \sigma_n^2 I_{nR}$, the denominator becomes independent of θ. Therefore, we can write:

$$\hat{f}_{dt}, \hat{f}_{st} = \max_{fd,fs} \left| \sum_{n=0}^{N-1} \sum_{m=0}^{n_T+n_R-2} f(n,m)\, e^{-j2\pi f_d n}\, e^{-j2\pi f_s m} \right|^2 \quad (73)$$

Where :

$$f(n,m) = \sum_{i=1}^{nT} x_i(n) r_{m+2-i}^{in}(n) \quad (74)$$

And :

$$r^{in}(n) = R_{in}^{-1} y(n) \quad (75)$$

As the number of samples is usually much larger than the number of transmitting and receiving antennas, i.e. $N \gg (n_T + n_R)$, the resolution of the Doppler frequency f_d is greater than the spatial frequency resolution f_s.

9. CONCLUSION

The MIMO radar concept differs from that of conventional radar by the use of several antennas both for transmission and reception, as well as by the particularity of the different waveforms transmitted. The main advantage of MIMO radar is spatial diversity, which has improved the system's capabilities compared to a radar system in terms of resolution, identification parameters, transmission beam synthesis and diversity gain. The performances in detection, localization and tracking of moving targets have shown that the integration of MIMO technology within the radar system offers better performance.

10. REFERENCES

[1] M. Stefano Fortuaniti, Luca Sanguineti,Fulvio Gini,Maria S.Greco,Braham Himed, *« Massive MIMO radar for target detection»,* IEEE,arXiv:1906.06191,15 Janvier 2020.

[2] M. Simon Foucart, Holger Rauhut *« A Mathematical introduction to compressive sensing »*, Drexel University Philadelpia et RWTH Aachen University,2010.

[3] M. Irena Orovic, Vladan Papic, Cornel Ioana, Xiumei Li, et Srdjan Stankovic *« Compressive Sensing in signals processing: algorithms and transform domain formulations »,* Hindawi Publishing Corporation-Mathematical Problems in Engineering,Article ID 7616393, 2 Aout 2016.

[4] M. Ravelomanantsoa Andrianiaina « Approche déterministe de l'acquisition comprimée et la reconstruction des signaux issus de capteurs intelligentes distribués », Université de Lorraine, 9 Novembre 2015.

[5] M. Zhen Gao, Linglong Dai, Wei Dai,Byonghyo Shim, et Zhaocheng Wang *« Structured compressive sensing-based spatio-temporal joint channel estimation for FDD massive MIMO »,* IEEE transactions on communications,Vol.64,NO.2,Fevrier 2016.

[6] M. Neda Rojhani, « Assessment of Compressive Sensing 2X2 MIMO Antenna Design for Millimeter-Wave Radar Image Enhancement », Université de Florence, 9 Avril 2020.

[7] M. Rauhut Holger *« Analysis of Compressive Sensing in Radar »*, RWTH Aachen University, 8 Decembre 2015.

[8]. M. Jungang Yang,Tian Jin, Chao Xiao, et Xiaotao *Huang « Compressed sensing radar imaging : fundamentals, challenges, and advances »,* College of Electronic Science and Technology, National University of Defense Technology, 13 Juillet 2019.

[9] M. Christopher Alan Rogers « MIMO radar waveform design and sparse reconstruction for extended target detection in clutter », Old Dominion University, Mai 2014.

[10] M. Magron Paul « Reconstruction de phase par modèles de signaux : application à la séparation de sources audio », Institut des Sciences et Technologie de Paris,2 Décembre 2016.

[11] M. Peng Chen, Zhenxin Cao, Zhimin Chen, Xianbin Wang *« Off-grid DOA estimation using sparse Bayesian learning in MIMO radar with unknown mutual coupling »,* IEEE transactions on signal processing, arXiv:1804.04460v3,7 Decembre 2018.

[12] M. Abdollah Ajorlo,Arash Amini, Mohamad H.Bastani *« A compressive sensing based colocated MIMO radar power allocation and waveform design »,* Journal of LATEX class files,Vol.14,NO.8, Août 2015.

[13] M. Shunqiao Sun *« MIMO radars with sparse sensing »* , The State University of New Jersey, Janvier 2016.